International Journal of Infrared and Millimeter Waves, Vol. 24, No. 9, September 2003 (© 2003)

SPURIOUS SIGNAL RESPONSE OF BROADBAND SOLID–STATE FREQUENCY MULTIPLIERS AT MILLIMETER AND SUBMILLIMETER WAVELENGTHS

Goutam Chattopadhyay, Frank Maiwald, Erich Schlecht, Robert J. Dengler, John C. Pearson, and Imran Mehdi

California Institute of Technology, Jet Propulsion Laboratory
329-47 Caltech, Pasadena, CA 91125, USA

Received July 1, 2003

Abstract

Heterodyne instruments at millimeter and submillimeter wavelengths often use wideband fixed-tuned frequency multipliers, in conjunction with broadband power amplifiers driven by frequency synthesizers, as the local oscillator (LO) source. At these frequencies the multipliers use Gallium Arsenide (GaAs) based Schottky varactor diodes as the nonlinear element, and like most other harmonic generators are susceptible to spurious signal interference. The state-of-the-art LO sources at these wavelengths use high power MMIC amplifiers at the initial stages, and are used to drive the subsequent multiplier stages to have enough LO power to pump the mixers. Because of the high input power environment and the presence of noise in the system, the multipliers become vulnerable to spurious signal interference. As the spurious signals propagate through the receiver system, they generate inter-modulation products which might fall in the passband of the heterodyne instrument and seriously degrade its performance. In this paper spurious signal response of solid-state frequency multipliers at millimeter and submillimeter wavelengths is investigated. Results of numerical harmonic balance simulations and laboratory experiments, which were found to show good agreement, are presented here.

Key Words

Spurious signals, frequency multipliers, millimeter and submillimeter wavelengths.

I. INTRODUCTION

Currently many new instruments, which are primarily intended for ground-based and space-borne astrophysical observations, are being built at millimeter and submillimeter wavelengths [1]–[3]. For high spectral resolution observations, heterodyne receivers (coherent detectors) are the receivers of choice for many of these instruments. In a heterodyne system, the incoming radio frequency signal (ν_{RF}) is down-converted to an intermediate frequency signal (ν_{IF}) in a mixer pumped by a local oscillator signal (ν_{LO}). At millimeter and submillimeter wavelengths, the first front-end component is a mixer, often cryogenic, such as superconductor insulator superconductor (SIS) or hot electron bolometer (HEB) mixers. Although the noise temperature of the mixer very often determines the overall noise temperature of a heterodyne receiver at these frequencies, noise contributions from other front-end components, such as the local oscillator (LO) and the intermediate frequency (IF) amplifiers cannot be ignored. At millimeter and submillimeter wavelengths, LO injection into the mixer is usually accomplished using either a waveguide coupler, a diplexer, or an optical beamsplitter. However, due to low available LO power, the coupling is fairly large, -10 dB or greater. This allows a significant amount of LO thermal noise to be injected into the receiver along with the LO signal, significantly increasing the receiver noise temperature. Apart from the LO thermal noise, the spectral purity of the LO signal also plays a major role in receiver performance. Often the LO amplitude noise or the phase noise show up in the passband of the IF signal, which increases the noise temperature of the receiver, resulting in degradation of the overall performance of heterodyne instruments. As a result, one requires a spectrally pure and low thermal noise LO system for a low noise heterodyne receiver.

LO systems at gigahertz (GHz) and terahertz (THz) frequencies have a variety of noise types associated with them. Apart from the thermal noise mentioned before, they have amplitude and phase noise which is due to the short time scale (< 1 s) zero-mean fluctuations in signal amplitude and phase, primarily caused by up-converted low frequency device noise. They have drift noise – which is due to the long time scale (> 1 s) fluctuations in amplitude and phase caused by temperature and other parameter changes. They also have spurious signal interference – which is due to the pick-up and propagation of spurious signals in a noisy environment, aided primarily by the nonlinear devices in the system. In this paper we look in closely at the spurious signal interference in solid-state frequency multipliers at millimeter and submillimeter wavelengths.

II. FREQUENCY MULTIPLIERS AND SPURIOUS SIGNALS

State-of-the-art broadband solid-state LO sources in the millimeter and submillimeter wavelengths are constructed from chains of cascaded Schottky

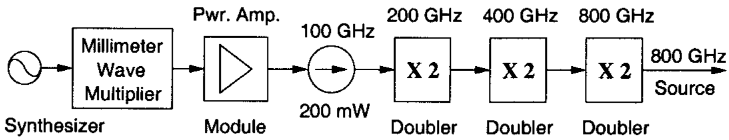

Fig. 1. Block diagram of a solid-state local oscillator chain using GaAs Schottky barrier varactor diode frequency multipliers. This specific chain was for 800 GHz output frequency, producing at about 1 mW of output power at room temperature [11].

barrier varactor diode frequency multipliers driven by frequency synthesizers and broadband monolithic millimeter wave power amplifiers [4]–[6]. Fig. 1 shows the block diagram of such a LO system working at 800 GHz. The signal from a frequency synthesizer is multiplied using a commercially available frequency multiplier module. This signal around 100 GHz is amplified using MMIC power amplifiers producing in excess of 250 mW [7]. This high power signal is then multiplied with a series of solid-state frequency multipliers to produce sufficient power at THz frequencies to adequately pump SIS or HEB mixers [8], [9].

The frequency multipliers at these frequencies use a novel planar substrateless technology in the fabrication of the Schottky barrier varactor diodes and various other on-chip matching circuits [10], [11]. Using conventional optical lithographic techniques and back-side wafer processing, free-standing metal beam leads are realized for DC and RF contacts and input and output coupling elements [12]. The units are constructed using split waveguide blocks where the multiplier chip rests on the split waveguide and the input signal is directly coupled to the diodes and the output signal is coupled to the output waveguide by means of an E-field probe.

Almost all studies concerning noise properties of frequency multipliers relate to close-in noise of the LO carrier [13], [14]. Most of the noise power of a frequency multiplied LO signal is generally concentrated in the close vicinity of the carrier, whose frequency slowly oscillates around an expected average value. This leads to the concept of fuzzy carrier and gives rise to noise sidebands. Phase noise measurement techniques are used to measure the close-in phase noise and noise sidebands. Allan variance measurements are done to determine the long term phase and amplitude drift of LO signals [14]–[16]. Moreover, linear analysis techniques of noise conversion have been developed over the years which can adequately predict the near-carrier noise properties, such as the amplitude and the phase noise, of typical frequency multipliers [17].

Less is reported about the far-from-carrier spurious interference properties of frequency multipliers in a LO system [18]. To produce enough pump power at the highest frequency stage of a multiplier chain, the first multiplier

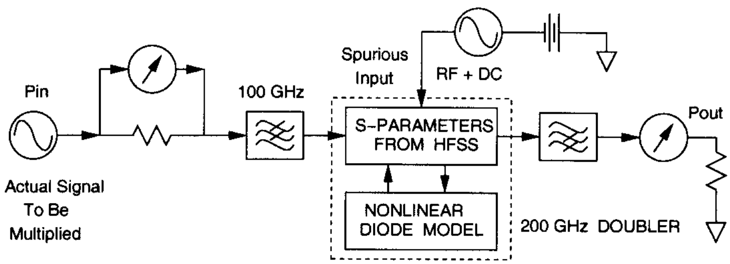

Fig. 2. Schematic diagram of the harmonic balance simulation setup used in ADS simulation. In this schematic the spurious signals are injected through the frequency multiplier DC bias line.

in the chain is often pumped with a high power input signal. Because of this high power environment and the fact that the multipliers and the driver amplifiers are very broadband, the frequency multipliers become vulnerable to spurious signal interference and can propagate out of band signals through the multipliers. As the spurious signals propagate through a chain such as the one shown in Fig. 1, they generate inter-modulation products which cannot be filtered out easily and may show up in the IF passband. Frequency multipliers can pick up spurious signals either through the DC bias lines or through the RF input port. The power amplifiers are also vulnerable to spurious signal interference which might propagate through to the input of the frequency multipliers, and in turn generate more spurious sidebands. These frequency multipliers often have on-chip bias filters which reject very high frequency noise signals on the bias lines, and also have external bias filters to reject low frequency noise signals from the multiplier bias. However, if not filtered properly, noise signals in the low GHz range can still leak through the bias lines of the multipliers and propagate to the output through inter-modulation products. These low GHz spurious signals are the major cause of concern because most of the heterodyne instruments currently being built in the millimeter and submillimeter wavelengths have IF frequencies in the low GHz range. We carried out numerical harmonic balance simulations and performed laboratory experiments to understand how the spurious signals propagate through a broadband solid-state frequency multiplier, and report the findings here. We confined our studies to spurious signals in the 1–5 GHz range and spurious signal interference through the multiplier DC bias line and through the RF input port.

III. NUMERICAL ANALYSIS AND EXPERIMENTAL SET-UP

We used Agilent's advanced design system (ADS) [19] nonlinear harmonic balance simulator to simulate the effect of spurious signal interference through the bias line and the RF input port of our 200 GHz frequency multiplier [10]. The frequency multiplier in question was a six-anode balanced doubler with 72 fF zero-bias diode junction capacitance. The schematic of the harmonic balance simulation we used in ADS is shown in Fig. 2. To design the 200 GHz frequency multiplier circuit we used the linear and the nonlinear circuit simulator of the ADS, and Ansoft's high frequency structure simulator (HFSS) [20] – a finite element 3-D electromagnetic field solver. For the spurious signal interference simulations of the multiplier, we used the nonlinear harmonic balance simulator of the ADS along with the S-parameters obtained from the HFSS simulations of the multiplier circuits in the waveguide structures, a nonlinear Schottky barrier varactor diode model [21], and a few other circuit elements such as lowpass, highpass, and bandpass filters, as shown in Fig. 2.

To simulate spurious signal interference through the bias line of the solid-state frequency multiplier, a single tone voltage source along with the DC bias was introduced at the multiplier bias input, as shown in Fig. 2. Before introducing the spurious signal through the bias line, the input pump power at 100 GHz was adjusted and the multiplier was optimally DC biased to generate about 20 mW of output power at 200 GHz. For our simulations we used 2 GHz and 5 GHz single tone spurious signals with different amplitude levels on the bias line input. The harmonic balance simulator was set up as a two-tone simulator with a maximum of three harmonics for each tone, and the maximum order was set to eight, allowing eight different mixing products to show up at the output along with the three harmonics of each of the tones.

For the simulations of spurious signal interference through the input port of the multiplier, the simulator was set up as a three-tone harmonic balance simulation with the center frequency at 100 GHz – the nominal input frequency, and two sidebands at either side of the carrier. Here again, before we introduced the spurious signals, the input power and the DC bias were adjusted to produce about 20 mW of output power at 200 GHz. For our simulations, we used two sets of sidebands, at ± 1 GHz and ± 2 GHz of the 100 GHz center frequency. In this particular simulation we used a maximum of two harmonics for each tone, as compared to three harmonics in the previous simulation, to facilitate convergence of the harmonic balance simulations. Here also the maximum order was set to eight, allowing eight different mixing products and two harmonics of each of the tones to show up at the output of the multiplier.

Fig. 3 shows the schematic diagram of the experimental set-up used for the measurements of the spurious signal interference through the bias line of the multiplier. The 100 GHz input signal for the multiplier under test was generated from a times six active frequency multiplier module pumped by a 16.67 GHz signal from a synthesizer. A WR-10 coupler connected to a calorimeter [22] was used to measure the input power to the multiplier at

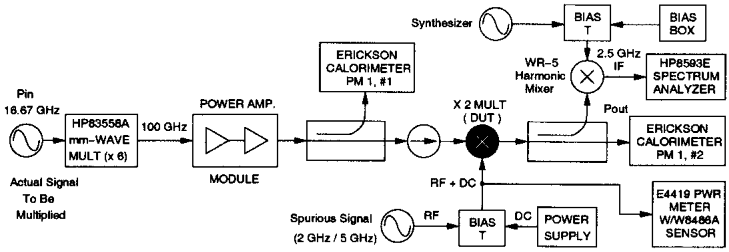

Fig. 3. Schematic diagram of the experimental set-up used for measuring spurious signal interference through the bias line of the 200 GHz balanced doubler. Spurious signals at 2 GHz / 5 GHz with different amplitude levels were injected in the bias line through the bias-T using a synthesizer shown at the bottom of the figure.

100 GHz. The power output from the frequency multiplier at 200 GHz was measured using another calorimeter connected through a WR-5 coupler. The output signal was down-converted to a 2.5 GHz IF by a WR-5 harmonic mixer and a synthesizer, as shown in Fig. 3. The frequency of the synthesizer used as the LO signal for the WR-5 harmonic mixer was adjusted to keep the IF output at 2.5 GHz at all times so that the IF calibration was required only at one frequency. The IF output from the harmonic mixer was measured using a spectrum analyzer as shown. A bias-T was used to DC bias the multiplier and also to inject the spurious signals through the bias line. The doubler was first optimally biased to generate maximum output power at 200 GHz and then a 2 GHz/5 GHz signal was injected into the bias-T as spurious input to the multiplier bias line.

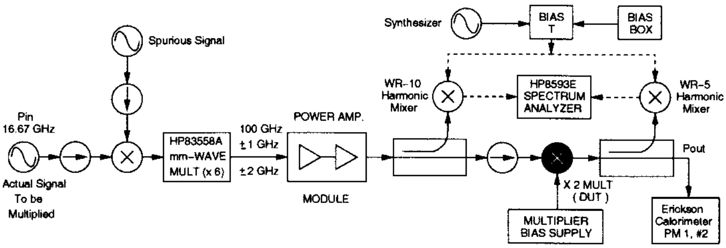

Fig. 4. Schematic diagram of the experimental set-up used for measuring spurious signal interference through the RF input port of the 200 GHz balanced doubler. Sidebands at ± 1 GHz and ± 2 GHz at 100 GHz carrier were injected using a mixer and a synthesizer at the input of the power amplifier module. The IF outputs from the WR-10 and WR-5 harmonic mixers are measured using a spectrum analyzer. The DC bias for the frequency doubler was kept fixed at the optimum bias level for this measurement.

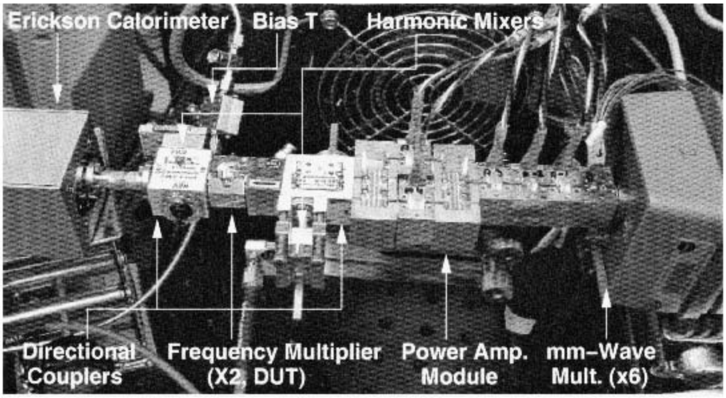

Fig. 5. Photo of our measurement set-up. On the right is the X 6 mm-wave multiplier which drives the power amplifier module at 100 GHz range. On the left is the Erickson calorimeter used to measure the output power from the 200 GHz balanced doubler.

Fig. 4 shows the schematic of the set-up used for spurious signal interference measurements through the RF input port of the frequency multiplier. For these measurements, we introduced spurious sidebands at ± 1 GHz and ± 2 GHz on the 100 GHz carrier signal using a mixer and a second synthesizer set at 15.67 GHz. The first synthesizer was set at 16.67 GHz, as in the previous measurement. The sideband levels at ± 1 GHz and ± 2 GHz spurious signals were controlled through the amplitude level of the second synthesizer. The 100 GHz input signal with sidebands was coupled to a WR-10 harmonic mixer which down-converted it to a 1.25 GHz IF signal and was measured using a spectrum analyzer. The output of the frequency multiplier was coupled to a WR-5 harmonic mixer which down-converted it to a 2.5 GHz IF signal and was measured with the spectrum analyzer. Before we started the experiments, both the input and the output signals at the through-port of the WR-10 and WR-5 couplers were measured with the calorimeter for calibration. The multiplier was biased to an optimum fixed DC value to get maximum power at 200 GHz. The LO frequencies for the harmonic mixers were adjusted in such a way that we always had 1.25 GHz IF output for all the sidebands of the WR-10 harmonic mixer output and 2.5 GHz IF output for all the sidebands of the WR-5 harmonic mixer output. As a result, we needed to calibrate the IF outputs only at 1.25 GHz and 2.5 GHz respectively. A photo of the measurement set-up we used for our experiments is shown in Fig. 5.

As a general calibration procedure, we characterized each and every individual components at all the relevant frequencies. The WR-10 coupler was calibrated at 100 GHz ±5 GHz with 1 GHz step size and the WR-5 coupler was calibrated at 200 GHz ±10 GHz with 1 GHz step size. The conversion loss of the WR-10 and WR-5 harmonic mixers was also measured with the RF power levels close to the signal levels used in the actual measurements.

IV. SIMULATION AND MEASUREMENT RESULTS

For simulations and measurements of spurious signal interference through the bias line of the frequency multiplier, we used a variety of signal amplitudes at 2 GHz and 5 GHz spurious signal input. Fig. 6 shows the simulated and the measured results of the 200 GHz frequency multiplier response to a 2 GHz, 185 mV pk-pk spurious signal through its bias port. It can be seen from the simulation results that the 2 GHz spurious signal has generated sidebands at ±2 GHz, ±4 GHz, and ±6 GHz of the 200 GHz multiplier output. The simulations predicted sideband levels at -36 and -39 dBc at 202 GHz and 198 GHz respectively. The other sidebands were found to be at -60 dBc or lower. The measured results shown on Fig. 6 were corrected for the conversion loss of the harmonic mixer and the WR-5. Given that the conversion loss of the harmonic mixer at 200 GHz was measured to be about 60 dB, and the noise floor of the spectrum analyzer was at -120 dBm (a combination of the resolution bandwidth, the video bandwidth, and the

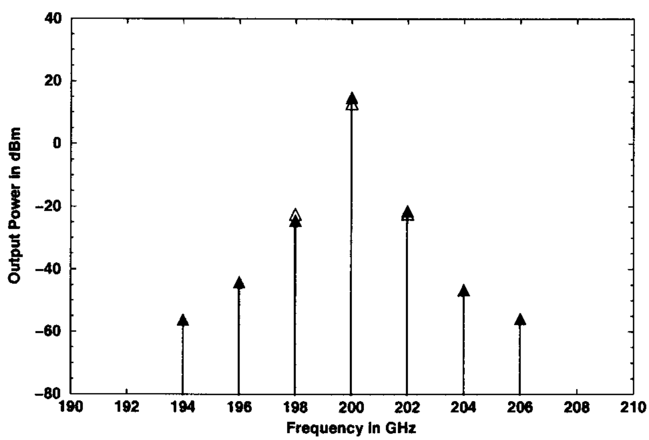

Fig. 6. Simulated and measured response of the 200 GHz frequency multiplier when a 2 GHz, 185 mV pk-pk spurious signal was introduced through the bias line of the multiplier. The filled triangles with solid lines are the simulated results and the open triangles with dotted lines are the measured results.

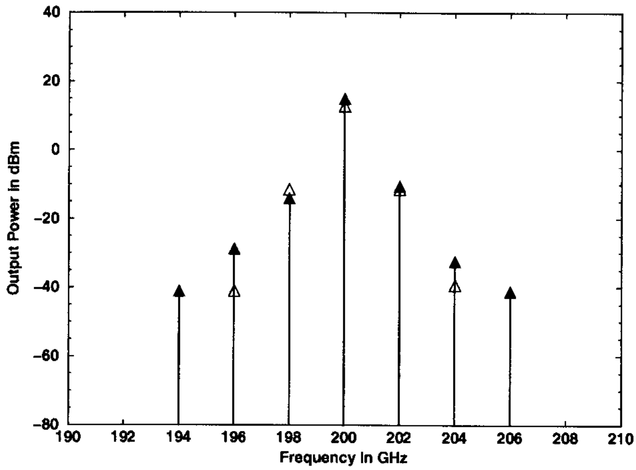

Fig. 7. Simulated and measured response of the 200 GHz frequency multiplier when a 2 GHz, 635 mV pk-pk spurious signal was introduced through the bias line of the multiplier. The filled triangles with solid lines are the simulated results and the open triangles with dotted lines are the measured results.

sweep-time of the spectrum analyzer set this limit), we could measure only one pair of sidebands, at ± 2 GHz of the 200 GHz carrier. Both the sidebands at 198 GHz and 202 GHz were measured to be at -35 dBc, which is about 4 dB and 1 dB higher than the corresponding simulated values. It can be seen from Fig. 7 that when we introduced a 2 GHz, 635 mV pk-pk spurious signal (10.7 dB higher than the previous input) on the bias line of the frequency multiplier, we measured sidebands at -24.4 and -24.2 dBc at 198 and 202 GHz respectively, which were about 11 dB higher than the previous case.

Fig. 8 shows the simulated and measured results when a 5 GHz, 200 mV pk-pk spurious signal was injected on the bias line of the multiplier. In this case, the measured sidebands were found to be about 3 and 1 dB higher than the corresponding simulated results at 195 and 205 GHz respectively. When we reduced the 5 GHz spurious signal amplitude by 10 dB (63 mV pk-pk), the sidebands were measured at -46.5 and -47.1 dBc at 195 and 205 GHz respectively, which were about 10 dB lower than the previous measurements. Fig. 9 shows the simulated and measured data for this case. We observed that the spurious sidebands at the output of the 200 GHz multiplier increased or decreased linearly with the amplitude level of the 2 GHz and the 5 GHz spurious inputs, till the multiplier reached saturation.

Fig. 10 shows the simulation and measurement results for spurious signal

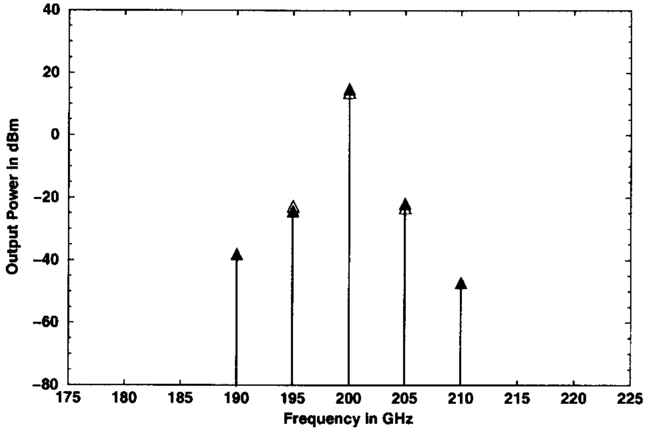

Fig. 8. Simulated and measured response of the 200 GHz frequency multiplier when a 5 GHz, 200 mV pk-pk spurious signal was introduced through the bias line of the multiplier. The filled triangles with solid lines are the simulated results and the open triangles with dotted lines are the measured results.

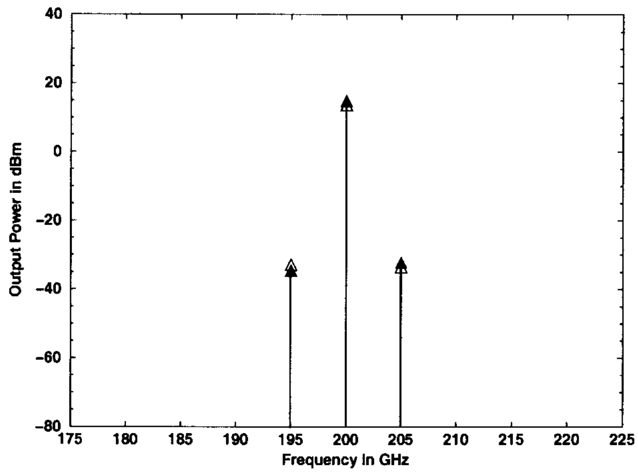

Fig. 9. Simulated and measured response of the 200 GHz frequency multiplier when a 5 GHz, 63 mV pk-pk spurious signal was introduced through the bias line of the multiplier. The filled triangles with solid lines are the simulated results and the open triangles with dotted lines are the measured results.

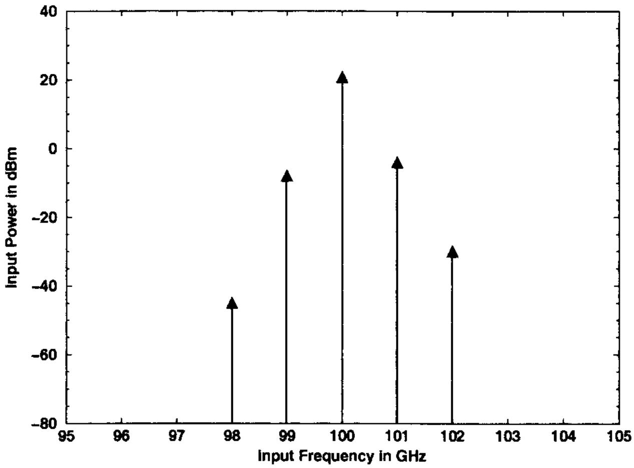

(a)

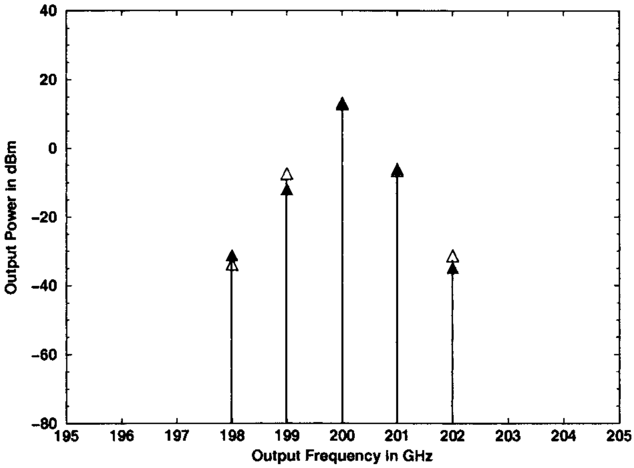

(b)

Fig. 10. Simulated and measured results for spurious signal interference through the RF input port of our 200 GHz frequency doubler. Fig. (a) shows the input signal used to pump the doubler and Fig. (b) shows the output at 200 GHz. The open and the close triangles are for simulated and measured results respectively.

interference through the RF input port of the frequency multiplier. Fig. 10(a) shows the input signal at 100 GHz with sidebands at ±1 GHz and at ±2 GHz, which was used to pump the frequency multiplier. Fig. 10(b) shows the simulated and measured results at the output of the 200 GHz frequency multiplier. When sideband levels at the 100 GHz pump signal were decreased by about 10 dB compared to the previous case (-38.8 and -34.8 dBc at 99 and 101 GHz respectively, the 100 GHz carrier level was kept the same), the output sidebands were measured at -30.2 and -29.2 dBc at 199 and 201 GHz respectively, which were about 10 dB lower than the previous measurements. Considering the machining tolerances of the multiplier blocks and the fabrication tolerances of the devices, simulation and measurement results show very good agreement. One should also notice that although the input had sidebands at ±1 GHz and at ±2 GHz at 100 GHz, the multiplier output produced sidebands ±1 GHz and at ±2 GHz at 200 GHz, because of the different mixing and inter-modulation products generated through the nonlinear frequency multiplier.

V. CONCLUSIONS

When a frequency multiplier experiences spurious signal interference, either through the bias line or through the RF input port of the multiplier, the signal is subjected to an input and output filter with symmetric diodes (because the multipliers are balanced) performing mixing of the signal with the input pump power and with the spurious signal itself. The conversion of the sidebands in a balanced varactor diode multiplier is highly dependent on the circuit design. Because of the inherent symmetry of the balanced circuit, the odd harmonic products are suppressed, depending on the degree of balance in the circuit.

We observed from the simulations and the measurements that when the spurious signal levels on the bias line of the multiplier are increased or decreased by about 10 dB, the sidebands at the output of the 200 GHz doubler increases or decreases by the same amount, till the doubler reaches saturation. We also noticed that a signal around 200 mV (pk-pk) in the 1–5 GHz range produces highest level sidebands in the -35 dBc level. We should remember that as these sidebands propagate through the multiplier chain, they will produce more sidebands, but will be at a lower level than the closest sidebands. However, other multipliers in the chain will produce their own sidebands due to spurious signal interference through their bias lines. To reduce these sideband levels, one needs to look into the bias filtering of the multiplier very closely. Incorporating bandstop filters in the bias line of the frequency multiplier in the IF frequency band will certainly help alleviate this problem.

As for the spurious signal interference through the RF input port, the output sideband levels change linearly with the change in the input sideband levels; when we decreased the input sideband levels by 10 dB, the output sideband levels also decreased by 10 dB. The spurious signal interference through the RF input port shows up slightly differently at the frequency multiplier output than the spurious signal interference through the bias line of the multiplier. We observed that sideband signals at ± 1 GHz of the 100 GHz input signal at -25 dBc level produces sidebands at ± 1 GHz of the 200 GHz output signal at -20 dBc, a 5 dB increase in the sideband levels from the input to the output. We expect a nominal 3 dB increase due to the multiplication factor – the multiplier in consideration here is a balanced doubler. However, we should keep in mind that these signal levels are very much dependent on the exact circuits used for the frequency multiplier. To reduce the spurious signal interference through the RF input port of the multiplier, one has to pay attention to the filters used on the bias line of the millimeter wave power amplifier modules.

ACKNOWLEDGMENTS

The authors would like to thank Peter Siegel of the Jet Propulsion Laboratory, and Jonas Zmuidzinas of the California Institute of Technology for their support. This work was carried out at the Jet Propulsion Laboratory, California Institute of Technology, Pasadena, California, USA, under contract with National Aeronautics and Space Administration.

REFERENCES

[1] G. L. Pilbratt, "The Herschel Mission, Scientific Objectives, and this Meeting," *Proceedings of "The Promise of the Herschel Space Observatory"*, eds. G. L. Pilbratt, J. Cermicharo, A. M. Heras, T. Prusti, and R. Harris, ESA SP–460, pp. 13–20, December 2000.

[2] R. L. Brown, "Technical Specification of the Millimeter Array," *Proceedings of SPIE:Advanced Technology MMW, Radio, and Terahertz Telescopes*, vol. 3357, pp. 231–237, Kona, March 1998.

[3] E. F. Erickson, J. A. Davidson, "SOFIA: The Future of Airborne Astronomy," *Proceedings of the Airborne Astronomy Symposium on the Galactic Ecosystem: From Gas to Stars to Dust*, eds. M. R. Haas, J. A. Davidson, and E. F. Erickson, San Francisco, April 1995.

[4] I. Mehdi, E. Schlecht, G. Chattopadhyay, and P. H. Siegel, "THz Local Oscillator Sources: Performance and Capabilities", *Proceedings of SPIE: Millimeter and Submillimeter Detectors for Astronomy*, vol. 4855, pp. 435–446, Waikoloa, Hawaii, USA, August 2002.

[5] N. R. Erickson, "Diode Frequency Multipliers for Terahertz Local-Oscillator Applications", *Proceedings of SPIE: Advanced Technology MMW, Radio, and Terahertz Telescopes*, vol. 3357, pp. 75–84, Kona, March 1998.

[6] P. Zimmermann, "Multipliers for THz Local Oscillators", *Proceedings of SPIE: Advanced Technology MMW, Radio, and Terahertz Telescopes*, vol. 3357, pp. 152–158, Kona, March 1998.

[7] L. A. Samoska, T. C. Gaier, A. Peralta, S. Weibreb, J. Bruston, I. Mehdi, Y. Chen, H. H. Liao, M. Nishimoto, R. Lai, H. Wang, and Y. C. Leong, "MMIC Power Amplifiers as Local Oscillator Drivers for FIRST", *Proceedings of SPIE: UV, Optical, and IR Space Telescopes and Instruments*, vol. 4013, pp. 275–284, San Diego, California, USA, August 2000.

[8] J. Zmuidzinas, J. W. Kooi, J. Kawamura, G. Chattopadhyay, B. Bumble, H. G. LeDuc, and J. A. Stern, "Development of SIS Mixers for 1 THz", *Proceedings of SPIE: Advanced Technology MMW, Radio, and Terahertz Telescopes*, vol. 3357, pp. 53–62, Kona, March 1998.

[9] W. R. McGrath, A. Skalare, B. S. Karasik, M. C. Gaidis, B. Bumble, H. G. LeDuc, P. J. Burke, R. Schoelkopf, D. E. Prober, "Superconductive Hot-Electron Mixers for Terahertz Heterodyne Receiver Applications", *Proceedings of SPIE: Advanced Technology MMW, Radio, and Terahertz Telescopes*, vol. 3357, pp. 14–21, Kona, March 1998.

[10] E. Schlecht, G. Chattopadhyay, A. Maestrini, A. Fung, S. Martin, D. Pukala, J. Bruston, and I. Mehdi, "200, 400 and 800 GHz Schottky Diode *Substrateless* Multipliers: Design and Results", *2001 IEEE MTT-S International Microwave Symposium Digest*, Phoenix, Arizona, USA, pp. 1649–1652, May 2001.

[11] G. Chattopadhyay, E. Schlecht, J. Gill, S. Martin, A. Maestrini, D. Pukala, F. Maiwald, and I. Mehdi, "A broadband 800 GHz Schottky Balanced Doubler", *IEEE Microwave and Wireless Components Letters*, vol. 12, no. 4, pp. 117–118, April 2002.

[12] S. Martin, B. Nakamura, A. Fung, P. Smith, J. Bruston, A. Maestrini, F. Maiwald, P. Siegel, E. Schlecht, and I. Mehdi, "Fabrication of 200 to 2700 GHz Multiplier Devices Using GaAs and Metal Membranes", *2001 IEEE MTT-S International Microwave Symposium Digest*, Phoenix, Arizona, USA, pp. 1641–1644, May 2001.

[13] E. W. Bryerton, D. L. Thacker, K. S. Saini, and R. F. Bradley, "Noise Measurements of YIG-tuned Oscillator Sources for the ALMA LO", *ALMA Memo No. 311*, NRAO, Charlottesville, Virginia, USA, August 2000.

[14] R. Ambrosini, "Measurements of Allan Variance and Short Term Phase Noise of Millimeter Local oscillators", *ALMA Memo No. 310*, NRAO, May 2000.

[15] D. L. Thacker, E. W. Bryerton, R. F. Bradley, and K. S. Saini, "Phase Drift Measurements of YIG-tuned Oscillator Sources for the ALMA LO", *ALMA Memo No. 311*, NRAO, Charlottesville, Virginia, USA, June 2001.

[16] J. W. Kooi, G. Chattopadhyay, M. Thielman, T. G. Phillips, and R. Schieder, "Noise Stability of SIS Receivers", *International Journal of Infrared and Millimeter Waves*, vol. 21, no. 5, pp. 689–716, May 2000.

[17] M. T. Faber, J. Chramiec, and M. E. Adamski, *Microwave and Millimeter-wave Diode Frequency Multipliers*, Artech House, Norwood, Mass., 1995.

[18] G. Chattopadhyay, E. Schlecht, F. Maiwald, R. J. Dengler, J. C. Pearson, and I. Mehdi, "Frequency Multiplier Response to Spurious Signals and its Effect on Local Oscillator Systems in Millimeter and Submillimeter Wavelengths", *Proceedings of SPIE: Millimeter and Submillimeter Detectors for Astronomy*, vol. 4855, pp. 480–488, Waikoloa, Hawaii, USA, August 2002.

[19] Advanced Design System (ADS), version 1.5, Agilent Technologies, 395 Page Mill Road, Palo Alto, CA 94304, USA.

[20] High Frequency Structure Simulator (HFSS), version 8, Ansoft Corporation, Four Square Station, Suite 200, Pittsburgh, PA 15219, USA.

[21] E. Schlecht, G. Chattopadhyay, A. Maestrini, D. Pukala, J. Gill, and I. Mehdi, "Harmonic Balance Optimization of Terahertz Schottky Diode Multipliers Using an Advanced Device Model", *Proceedings of the Thirteenth International Symposium on Space Terahertz Technology*, Cambridge, MA, USA, pp. 187–196, March 2002.

[22] N. R. Erickson, "A Fast and Sensitive Submillimeter Waveguide Power Meter", *Proceedings of the Tenth International Symposium on Space Terahertz Technology*, University of Virginia, Charlottesville, Virginia, USA, pp. 501–507, March 1999.